

# Augmentation of Power Output of Axisymmetric Ducted Wind Turbines by Porous Trailing Edge Disks

Sheila Widnall, James Byron and Peter Florin

Massachusetts Institute of Technology

July 2014

## Introduction

This paper presents analytical and experimental studies of the augmentation of a ducted wind turbine by the addition of a porous disk placed at the trailing edge plane, as shown in Figure 1. The results show a perhaps surprising increase in power output from the placement of a rather simple device, a porous disk which can be constructed by simply placing holes in a solid disk to achieve a desired drag coefficient.

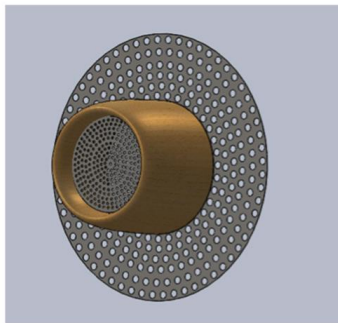


Figure 1: Duct with Trailing Edge Porous Disk

However, there are other intriguing possibilities. Another possibility is to design a porous disk whose drag coefficient can be changed by simple geometric means. Such a device could aid in the spin-up of the turbine in low wind conditions, and could moderate its speed at high wind speeds, making the device more flexible in changing wind conditions.

Figure 2 shows an adjustable porous disk device consisting of two layers of radial slats; the porosity of the disk can be changed by simply rotating the layers of slats relative to one another.

Wind tunnel tests were performed to measure the change in power output from the addition of a porous trailing edge device to the trailing edge of a ducted wind turbine. The experimental results agree with analytical predictions: the addition of a porous trailing edge device produces a significant increase in power output for a very simple and relatively inexpensive addition to the geometry of the device.

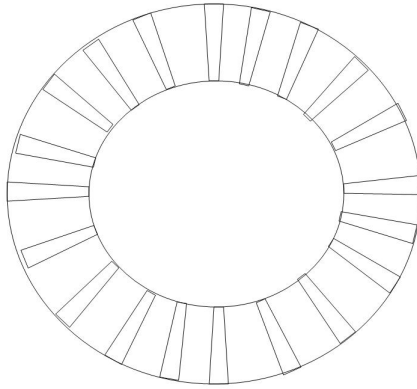


Figure 2: Geometric Modification of Porosity

## Analysis

In a previous paper, "Potential Flow Calculations of Axisymmetric Ducted Wind Turbines"; DSpace@MIT; an incompressible potential-flow vortex method was constructed to analyze the flow field of a ducted wind turbine. In this method, vortex panels were used to define the shape of the duct and to account for the flow changes due to the pressure drop across the turbine disk. This model moved beyond the one-dimensional flow models in which the pressure at the trailing edge, which is a key variable, is assumed to be atmospheric.

It may seem surprising that potential flow can be used to describe the flow of a ducted wind turbine, but under the assumption of uniform changes in static and stagnation pressure across the turbine disk, as is done in the Betz model, both regions of the flow have a potential function. The velocity field, which is irrotational, is unchanged across the actuator disk. The two regions of flow are defined by the stagnation pressure change across the actuator disk and by the cylindrical vortex sheet that originates from the trailing edge of the duct as a result of the pressure changes across the disk.

In experiments in which the actuator disk is replaced by a uniform screen, the change in stagnation pressure is not likely to be constant across the actuator disk due to the non-uniform velocity at the disk entry. This calls into question the use of screens to represent an actuator disk across which the change in stagnation pressure is assumed to be constant. However, these errors are of the same order as the application of actuator disk theory itself to a problem as complex as a wind turbine with a finite or an infinite number of blades. In any case this potential flow model should be considered to be a descendent of the Betz model and other similar analysis of ducted propellers and should give useful insights into the operation of ducted wind turbines.

The advantages of such a simplified model are that basic questions can be investigated without the complexity of a full CFD simulation: basic questions such as the momentum balance in the flow; the forces acting on the duct; the role of the Kutta condition in comparison to its usual form for an airfoil in a uniform

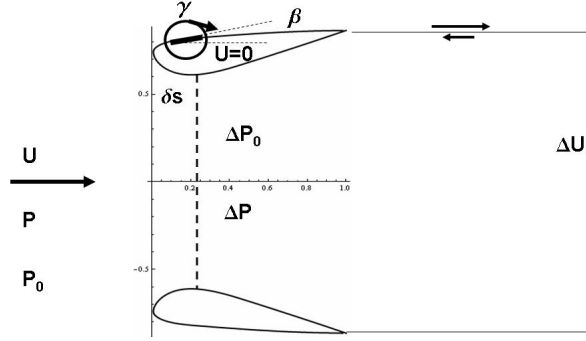


Figure 3: Geometry of Airfoil/Duct

potential flow; the interaction between the external and the internal flows, and the circulation about the airfoil/duct. This model moves beyond the assumptions of one-dimensional flow in the throat and at the exit of the duct as well as the assumption of atmospheric pressure at the exit.

However, a potential flow model fails to identify possible flow separation due to viscous effects in the duct diffuser. Therefore, it must be applied to duct designs whose separation possibilities are unlikely. In any case, it can serve as a first cut at understanding.

In this paper, this analysis is extended to study the augmentation of power output by the addition of trailing edge devices, in this case a porous disk placed at the exit plane. This idea follows a previous patent (Ohya et al.) in which a solid brim was placed at the exit; this modification increased the power output of the turbine.

However, a solid brim leads to flow separation and the occurrence of unsteady vortex shedding. The question we ask is whether a porous disk could augment turbine power, while leading to a steadier, more controllable flow in the wake of the duct.

In addition, a major advantage of a porous disk is its potential adjustability. The system can be designed to respond to changing wind conditions, adjusting the porosity of the disk geometrically in a manner to optimize the configuration for different wind speeds. At very low wind speeds, lower porosity, higher drag, can aid in startup by increasing velocity through the duct. While at higher wind speeds, higher porosity, lower drag, can reduce the velocity through the duct and decrease the load on the turbine, and varying the rpm as desired.

### Axisymmetric Ducts by Vortex Methods

In the previous analysis, vortex panels were used to represent the flow on the airfoil-like duct.

For the axisymmetric duct configuration in a free stream, the application of vortex methods to determine the potential flow solution is straightforward. For a wind turbine or ducted propeller, an additional consideration must be given to the stagnation-pressure discontinuity across the actuator disk. This results in a velocity discontinuity –or vortex sheet–originating from the trailing edge of the airfoil/duct. It also gives

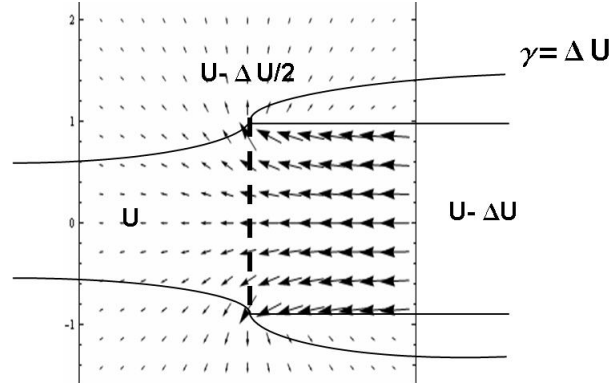


Figure 4: Flow Field of the Betz Model

rise to questions about the form of the Kutta condition to be applied to the configuration shown in Figure 3.

For a ducted turbine an additional component of the flow field is the semi-infinite vortex wake in the three-dimensional axisymmetric flow, as shown in Figure 4. The total solution for the actuator disk problem is obtained by adding a free stream of velocity  $U$  to the vortex wake solution. (The form of these solutions is given in an appendix of the previous paper for both two-dimensional and axisymmetric flow.) In both cases, both the horizontal velocity  $U$  and the vertical velocity  $V$  are continuous—and irrotational—across the “disk”. The  $U$  velocity in the far downstream wake is  $U - \Delta U$ . And the change in  $U$  velocity at the disk is uniform and exactly equal to  $1/2$  of  $\Delta U$ . Of some interest is that the vertical velocity  $V$  is not zero on the disk but has a logarithmic singularity near the upper edge. When this  $V$  velocity is integrated from  $-\infty$  to  $+\infty$ , a good approximation for the shape of the Betz bounding streamline is obtained.

The vortex sheet experiences a vertical self-induced velocity, both upstream and downstream of the disk, which will transport the sheet causing it to assume the proper curved shape. However, this effect should have little effect on the velocity field induced at the actuator disk. From this simple model of the semi-infinite vortex sheet shown in Figure 4, momentum change and power extraction can be calculated, leading to the Betz model for wind turbine performance.

### Power Augmentation by a Porous Disk

The model assumed in the previous paper considered the three-dimensional “airfoil” duct represented by a vortex panel distribution on the airfoil surface, supplemented with the vortex sheet that is created at the trailing edge due to the loss in stagnation pressure caused by the power extraction by the turbine. Consistent with the Betz model, the change in stagnation pressure was taken as constant across the disk.

In the previous paper it was demonstrated how the velocity field from the vortex sheet emanating from the trailing edge, due to loss in stagnation pressure in the duct flow due to power generated by the turbine, could be incorporated into the potential flow formulation of airfoil pressure distribution. Important in this

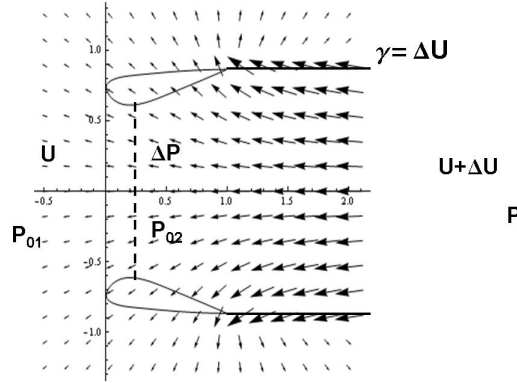


Figure 5: Flow Field and Geometry of Airfoil/Duct with Vortex Sheet

analysis was the imposition of the Kutta condition. Treating the duct as an axisymmetric airfoil, we imposed the Kutta condition: equal static pressure at the trailing edge in the upper and lower flows. The actuator disk, its accompanying vortex wake and its effect on flow field of the airfoil/duct through the velocity field induced by the vortex wake is incorporated into the method of Lewis. For a free stream velocity,  $U_\infty = 1$ , the velocity far downstream in the wake is given by  $1 - \Delta$ . The velocity field seen by the airfoil for the velocity change of  $-\Delta$  is given by  $U_w(x, y)$  and  $V_w(x, y)$  (or  $x, r$ ) as given in the appendix of the previous paper for both two- and three -dimensional flows.

Figure 5 shows the velocity field experienced by the duct as a result of the trailing vortex sheet. Since the airfoil is also a vortex sheet, the airfoil boundary condition will interact with the velocity due to the vortex sheet, resulting in a satisfaction of the airfoil boundary condition, leaving a "Betz" vortex wake beginning at the trailing edge. The incorporation of the vortex wake due to stagnation pressure loss in the duct, as done in the previous paper, was thus straightforward. The previous paper goes on to calculate the flow, the lift and drag forces, and the power output of the ducted turbine.

For a ducted wind turbine with a vortex sheet, the Kutta condition is applied as follows. For a vortex sheet strength of  $\Delta$  (normalized by the free stream velocity  $U = 1$ ), the velocity in the "free-stream" flow emerging from the duct is  $U_1 = 1 - \Delta$ . The fluid density is taken as  $\rho = 1$ . Thus the change in stagnation pressure is  $p_{01} - p_{02} = \Delta - \Delta^2/2$ . The Kutta condition, that the static pressure at the trailing edge in the upper and lower flow are equal,  $p_{u_{te}} - p_{l_{te}} = 0$ , results in the requirement that

$$1/2u_{u_{te}}^2 - 1/2u_{l_{te}}^2 = \Delta - \Delta^2/2. \quad (1)$$

In the previous analysis of the potential flow field of a ducted turbine, this boundary condition was applied at the trailing edge of the "airfoil" duct.

We now consider the addition of a porous disk to the trailing edge of the duct. It is now quite clear how to incorporate the effect of a porous disk place at the trailing edge. Assuming constant stagnation pressure

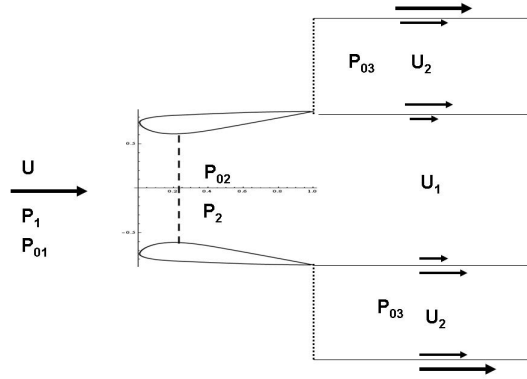


Figure 6: Flow Field and Geometry of Airfoil/Duct with Vortex Sheet

drop across the porous disk, an additional vortex sheet is added to the flow, as shown in Figure 6, and its velocity field acts upon the airfoil boundary condition, changing the overall potential flow solution. Key to the augmentation of power due to the porous disk is its effect upon the Kutta condition. Since the pressure behind the disk is reduced, the pressure at the outlet of the duct is also reduced. This increases the mass flow through the duct and thus increases the power output of the turbine.

We describe the strength of the vortex sheet shed from the porous disk as  $U_\infty - U_2 = \Delta_D$  where again we take  $U_\infty = 1$  and  $\rho = 1$  to normalize our solution. Describing the flow far downstream of the duct, we would again have a flow of constant static pressure in the various flow regimes:  $p_1 = p_2 = p_3$ . We write the expressions for the stagnation pressure in terms of the strength of the vortex sheets.

$$p_{01} = p_1 + 1^2/2 \quad (2)$$

$$p_{02} = p_2 + (1 - \Delta)^2/2 = p_{l_{te}} + 1/2u_{l_{te}}^2 \quad (3)$$

$$p_{03} = p_3 + (1 - \Delta_D)^2/2 = p_{u_{te}} + 1/2u_{u_{te}}^2 \quad (4)$$

where  $p_{u_{te}}$  and  $p_{l_{te}}$  are the static pressures at the upper and lower parts of the trailing edge where the Kutta condition is applied. This results in the Kutta condition

$$1/2u_{u_{te}}^2 - 1/2u_{l_{te}}^2 = \Delta - \Delta^2/2 - \Delta_D + \Delta_D^2/2 \quad (5)$$

This boundary condition replaces Equation (13) of the previous paper.

The velocity field experience by the airfoil now contains two velocity components due to the two trailing vortex sheets as shown in Figure 7. These additional velocity disturbance are incorporated into Lewis's method to determine the potential flow solution. The strengths of the two vortex sheets are related to the velocity change across them. We define these vortex strengths as  $\Delta$  and  $\Delta_D$ . These are the independent parameters in the analysis.

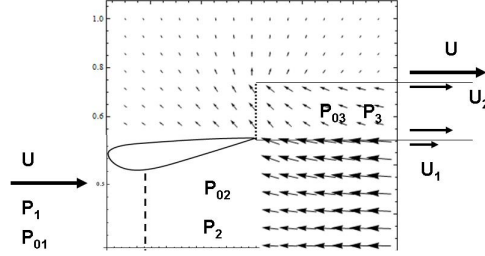


Figure 7: Flow Field and Geometry of Airfoil/Duct with Porous Disk Modeled by Vortex Sheets

## Results

Following the methods of the previous paper, calculations were done to determine the power output of two ducted turbines: with a porous disk placed on the exit plane of radius 1.5; and a porous disk of radius 2.5, relative to the *exit* radius of the duct. The flow field was modeled by representing the disk with an additional vortex sheet. Calculations were done for an annular duct of area ratio 2 with an airfoil shape as shown in Figure 3. A variety of porous disks, characterized by the strength of the vortex sheet,  $\Delta_D$ , generated by the stagnation pressure drop across the disk, were placed at the trailing edge of the duct. A variety of  $\Delta'_D$ 's were chosen: 0, .2, .4, .6, .7, .8, .9. For each case, a variety of non-dimensional duct-wake velocity changes  $\Delta'$ 's ( $U_{duct-wake} = 1 - \Delta$ ) due to the rotor disk were examined from  $\Delta = 0$  to  $\Delta = .8$ .

Power extracted was calculated and compared with the Betz values for an actuator disk of the same area as the duct throat, taken as unity. Power extraction is given by stagnation pressure (or static pressure) loss across the disk times throat velocity and throat area. The non-dimensionalized power extraction coefficient  $c_{\Pi}$ , or efficiency, is then

$$c_{\Pi} = \frac{(p_{01} - p_{02})}{\frac{1}{2}\rho U_{\infty}^3} U_t \quad (6)$$

where  $U_t$  is the velocity at the throat. As discussed in the previous paper, the throat velocity calculated by a potential flow model is not constant across the duct, but is a maximum at the airfoil surface. The value of this velocity is typically 10% above the average throat velocity. Given the simplicity of our model, we will simply use this value for throat velocity.

Figure 8 and Figure 9 show the non-dimensionalized power coefficients extracted by a ducted turbine of unit area in a duct of area ratio 2 as a function of the non-dimensionalized change in wake velocity  $\Delta U_1 = \Delta$  for a variety of porous trailing edge disks characterized by the non-dimensional change in the wake velocity  $\Delta U_2 = \Delta_D$ .  $\Delta_D = 0$  is the result for a ducted turbine without a porous disk at the trailing edge. Also shown (dashed) is the power extracted by an isolated actuator disk of unit area from the simple Betz model.

For the radius of the porous disk equal to both  $R_D = 1.5R$  and  $R_D = 2.5R$ , the augmentation of power output by the addition of porous disk is dramatic. Also, perhaps surprisingly, the power output is nearly the same for both of these cases. The power results also show that the maximum power occurs at higher values of the vortex sheet strength  $\Delta$  than for an actuator disk turbine in a free stream. These results

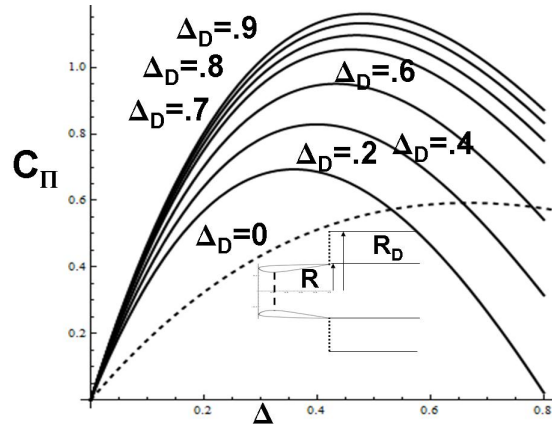


Figure 8: Total Power Coefficient  $C_{\Pi}$  With Various Porous Disks  $\Delta_D$  of Radius  $R_D = 1.5R$  vs.  $\Delta$  Wake Velocity: Ducted Wind Turbine and Betz Model

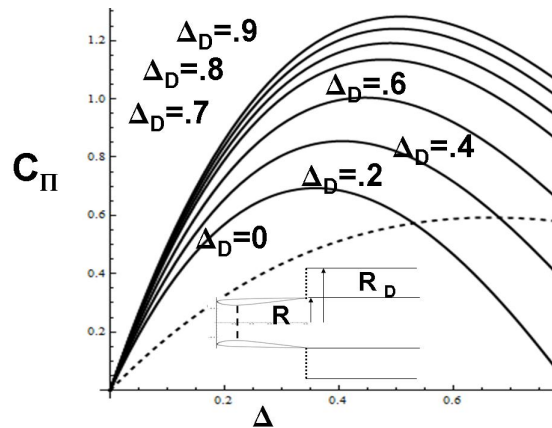


Figure 9: Total Power Coefficient  $C_{\Pi}$  With Various Porous Disks  $\Delta_D$  of Radius  $R_D = 2.5R$  vs.  $\Delta$  Wake Velocity: Ducted Wind Turbine and Betz Model

indicated that power output from a ducted turbine can be dramatically increased by placing a porous disk at the downstream edge of the duct.

The variation of power output with porosity also indicates that power output can be varied by changing the geometry of the downstream disk to change its effective porosity i.e. its drag and pressure loss parameters. This variability will be useful allowing it to respond to changes in wind velocity in an optimum manner.



Questions remain about the application of potential flow to a ducted turbine modeled as an actuator disk or to an experiment in which uniform screens are used to model the disk, since it is unlikely that the pressure drop across the actuator disk would be constant with a non-uniform flow entering the disk. However, this modeling defect is related to many of the issues in modeling a wind turbine by an actuator disk. Even in the face of this, the potential flow gives useful insights and valuable results.

## Experimental Results

Experiments to measure the power output of a ducted turbine augmented by the addition of a porous disk placed at the trail edge were carried out in the Wright Bros Wind Tunnel at MIT. The duct had a diameter

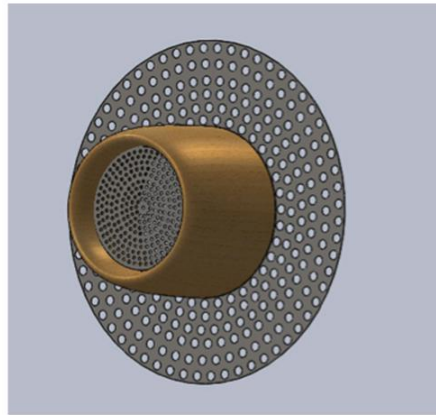


Figure 10: Experiential Wind Tunnel Model

of 11 inches and a profile using a NACA 2316 airfoil with a six degree half angle relative to the centerline and an area ratio of two. Circular mesh screens of varying mesh porosity were place at the centerline to simulate the pressure drop and power extraction by a wind turbine placed at the throat of the duct. The pressure drop across the screen was measured using a pitot tube. Experiments were conducted at a flow speed of 50mph.

The trailing edge porous brim was attached to the trailing edge of the duct. The inner diameter of the disk, which was equal to the outer diameter of the exit of the duct was 11 inches. Porous disks of various porosities and of a diameter of 22 inches were used in the experiment to simulate the trailing edge devices. The experimental results are shown in Figure 11. The results are presented as the power coefficient  $C_P$  as

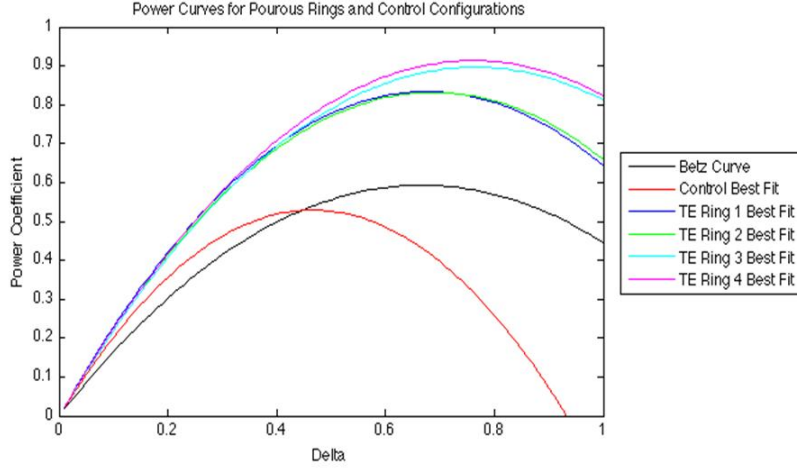


Figure 11: Experimental Results

a function of the non-dimensional velocity drop  $\Delta$  across the duct.

$$C_P = \frac{(p_1 - p_2)\dot{m}}{\frac{1}{2}A_T V_\infty^3} = \frac{2(p_1 - p_2)V_T}{V_\infty^3} \quad (7)$$

$$\Delta = 1 - \frac{V_2}{V_\infty} \quad (8)$$

Nine throat screens of different porosities were tested. As a control, the duct and its throat screens were tested without the accompanying porous trailing edge disk, as a traditional ducted wind turbine. The porous training edge disk was varied for zero percent (a solid flat plate) to 40% porosity. Roughly 100 data points were collected for each case. The final results were fitted to a smooth curve. Figure 11 shows the control, the power coefficient for the duct without the porous trailing edge. It also shows the theoretical Betz curve for comparison. The control is somewhat below the theoretical Betz curve as would be expect for a wind tunnel test. The remaining curves show the power coefficient for a variety of porous disks. The results show that the additional of a porous trailing edge disk almost doubles the power output for the control duct. Thus the analytical predictions are verified.

## References

- Widnall, S.E., **Potential Flow Calculations of Axisymmetric Ducted Wind Turbines**, *dspace.mit.edu/handle/1721.1*  
2009
- Lewis, R.I., **Vortex Element Methods for Fluid Dynamic Analysis of Engineering Systems**,  
Cambridge Engine Technology, Cambridge University Press 1991
- Ohya et al., **Wind Power Generator**, Patent No. US 6,756,696 B2, June 2004